Manuscript Number: COST-D-15-02074R1

Title: Testing and analysis of pultruded GFRP continuous beams for the deflection serviceability limit state

Article Type: Full Length Article

Keywords: GFRP; multi-span beams; pultrusions; serviceability deformations; shear-deformation analysis; testing

Corresponding Author: Dr Geoffrey Turvey,

Corresponding Author's Institution: Lancaster University

First Author: Geoffrey Turvey

Order of Authors: Geoffrey Turvey

Abstract: An investigation of the deformation response of an unequal two-span pultruded glass fibre reinforced polymer (GFRP) wide flange (WF) beam up to the deflection serviceability limit is described. The beam was subjected to vertical point loading at the centre of the longer span. Mid-span deflections, support rotations and outer surface flange strains recorded during major- and minor-axis flexure tests on the beam are presented and shown to be both repeatable and linear. New closed-form shear deformation equations are presented for the forces and displacements of two-span continuous beams of arbitrary span ratio with the longer span subjected to a vertical mid-span point load. The equations have been used to predict the mid-span deflections, support rotations and surface strains recorded during the flexure tests. It is shown that the equations are able to predict the experimental deflections accurately. Depending on the particular support, the rotations (particularly the minor-axis rotations) are slightly under/over-estimated and, in general, the surface strains are over-estimated. It is concluded that this investigation provides further confirmation of the utility of shear deformation continuous beam equations for predicting the serviceability deformations of pultruded GFRP beams up to the deflection serviceability limit.

Response to Reviewers: Date: Dec 28, 2015
To: "Geoffrey Turvey" g.turvey@lancaster.ac.uk
cc: ;null
From: "Composite Structures" cost@elsevier.com
Subject: Your Submission
Ms. Ref. No.: COST-D-15-02074
Title: Exact Shear-Deformation Analysis and Serviceability Testing of Pultruded GFRP Continuous Beams
Composite Structures

Dear Dr Geoffrey Turvey,

The reviewers have commented on your above paper. They indicated that it is not acceptable for publication in its present form.

However, if you feel that you can suitably address the reviewers' comments (included below), I invite you to revise and resubmit your manuscript.

Please carefully address the issues raised in the comments.

If you are submitting a revised manuscript, please also:

a) outline each change made (point by point) as raised in the reviewer comments

AND/OR

b) provide a suitable rebuttal to each reviewer comment not addressed

To submit your revision, please do the following:

1. Go to: http://ees.elsevier.com/cost/

2. Enter your login details

3. Click [Author Login]
This takes you to the Author Main Menu.

4. Click [Submissions Needing Revision]

Please note that this journal offers a new, free service called AudioSlides: brief, webcast-style presentations that are shown next to published articles on ScienceDirect (see also http://www.elsevier.com/audioslides). If your paper is accepted for publication, you will automatically receive an invitation to create an AudioSlides presentation.

Composite Structures features the Interactive Plot Viewer, see: http://www.elsevier.com/interactiveplots. Interactive Plots provide easy access to the data behind plots. To include one with your article, please prepare a .csv file with your plot data and test it online at http://authortools.elsevier.com/interactiveplots/verification before submission as supplementary material.

I look forward to receiving your revised manuscript.

Yours sincerely,

Antonio J. M. Ferreira
Editor
Composite Structures

Note: While submitting the revised manuscript, please double check the author names provided in the submission so that authorship related changes are made in the revision stage. If your manuscript is accepted, any authorship change will involve approval from co-authors and respective editor handling the submission and this may cause a significant delay in publishing your manuscript

Reviewer #1: Journal name
Composite Structures

Paper title
Exact Shear-Deformation Analysis and Serviceability Testing of Pultruded GFRP Continuous Beams

Authors
G. J. Turvey

General comments
An investigation of the serviceability behaviour of unequal two-span pultruded glass fibre reinforced polymer (GFRP) beams subjected to vertical point loading at the centre of the longer span is described. Mid-span deflections, support rotations and outer surface flange strains for major- and minor-axis flexure tests on a pultruded glass fibre reinforced polymer (GFRP) Wide Flange (WF) beam are presented and shown to be both repeatable and linear. New closed-form shear deformation equations are presented for the forces and displacements of two-span continuous beams of arbitrary span ratio with the longer span subjected to a vertical mid-span point load. The equations have been used to predict the mid-span deflections, support rotations and surface strains recorded in the beam tests. It is shown that the equations are able to predict the experimental deflections accurately. Depending on the particular support, the rotations (particularly the minor-axis rotations) are slightly under/over-estimated and, in general, the surface strains are over-estimated. It is concluded that this investigation provides further confirmation of the utility of shear deformation continuous beam equations for predicting the serviceability deformations of pultruded GFRP beams.
In the review's opinion the object of the paper presents a new contribution and the numerical and experimental results do provide additional knowledge and understanding on the mechanical behavior of continuous GFRP beams.
The quality of writing is clear.
I recommend the publication on the journal with major revision.

Specific comments

1) In order to update the introduction relative to studies on the flexural testing of GFRP beams, I suggest also to introduce a recent paper published in Composite Structures

Ascione F , Mancusi G, Spadea S, Lamberti M, Lebon F, Maurel-Pantel A. On the flexural behavior of GFRP beams obtained by bonding simple panels: an experimental investigation. Composite Structures 2015; 131: 55-65

2) I suggest to give more information about the GFRP beams: producer and all the mechanical parameters (transversally isotropic material);

3) I suggest to give more information about the experimental set-up. In details, the force passes through the centroid of the cross section? In order to evaluate the global flexural response of the beam how have

you contrast the possible cracks close to the zone in which the force is applied?

4) The load you declare in the paper is refereed to serviceability limit state (then under this load the response of the beam should be linear elastic). For this kind of beams (GFRP) the literature declares that the behavior is linear elastic up to failure. Really, this is not always the truth because of in the web/flange connection of the pultruded beams there is a resin concentration (depending on the pultrusion process) that provokes a gradual variation of the flexural stiffness. See papers:

Mosallam AS, Elsadek AA, Pul S. Semi-rigid behaviour of web-flange junctions of open-web pultruded composites. Proceedings of the international conference on FRP composites 2009, San Francisco, California. 2009.

Feo L, Mosallam AS, Penna R. Mechanical behavior of web-flange junctions of thin-walled pultruded I-profiles: an experimental and numerical evaluation. Compos: Part B 2013;48:18-39.

Have you take into account this aspect in your analysis? Which is the failure load of the beams tested?

5) I suggest, if possible, to insert graphs relative to the load-displacements curves.

Reviewers' comments:

Reviewer #1: Journal name
Composite Structures

Paper title
Exact Shear-Deformation Analysis and Serviceability Testing of Pultruded GFRP Continuous Beams

Authors
G. J. Turvey

General comments
An investigation of the serviceability behaviour of unequal two-span pultruded glass fibre reinforced polymer (GFRP) beams subjected to vertical point loading at the centre of the longer span is described. Mid-span deflections, support rotations and outer surface flange strains for major- and minor-axis flexure tests on a pultruded glass fibre reinforced polymer (GFRP) Wide Flange (WF) beam are presented and shown to be both repeatable and linear. New closed-form shear deformation equations are presented for the forces and displacements of two-span continuous beams of arbitrary span ratio with the longer span subjected to a vertical mid-span point load. The equations have been used to predict the mid-span deflections, support rotations and surface strains recorded in the beam tests. It is shown that the equations are able to predict the experimental deflections accurately. Depending on the

particular support, the rotations (particularly the minor-axis rotations) are slightly under/over-estimated and, in general, the surface strains are over-estimated. It is concluded that this investigation provides further confirmation of the utility of shear deformation continuous beam equations for predicting the serviceability deformations of pultruded GFRP beams.
In the review's opinion the object of the paper presents a new contribution and the numerical and experimental results do provide additional knowledge and understanding on the mechanical behavior of continuous GFRP beams.
The quality of writing is clear.
I recommend the publication on the journal with major revision.

Specific comments

1) In order to update the introduction relative to studies on the flexural testing of GFRP beams, I suggest also to introduce a recent paper published in Composite Structures

Ascione F , Mancusi G, Spadea S, Lamberti M, Lebon F, Maurel-Pantel A. On the flexural behavior of GFRP beams obtained by bonding simple panels: an experimental investigation. Composite Structures 2015; 131: 55-65

2) I suggest to give more information about the GFRP beams: producer and all the mechanical parameters (transversally isotropic material);

3) I suggest to give more information about the experimental set-up. In details, the force passes through the centroid of the cross section? In order to evaluate the global flexural response of the beam how have you contrast the possible cracks close to the zone in which the force is applied?

4) The load you declare in the paper is refereed to serviceability limit state (then under this load the response of the beam should be linear elastic). For this kind of beams (GFRP) the literature declares that the behavior is linear elastic up to failure. Really, this is not always the truth because of in the web/flange connection of the pultruded beams there is a resin concentration (depending on the pultrusion process) that provokes a gradual variation of the flexural stiffness. See papers:

Mosallam AS, Elsadek AA, Pul S. Semi-rigid behaviour of web-flange junctions of open-web pultruded composites. Proceedings of the international conference on FRP composites 2009, San Francisco, California. 2009.

Feo L, Mosallam AS, Penna R. Mechanical behavior of web-flange junctions of thin-walled pultruded I-profiles: an experimental and numerical evaluation. Compos: Part B 2013;48:18-39.

Have you take into account this aspect in your analysis? Which is the failure load of the beams tested?

5) I suggest, if possible, to insert graphs relative to the load-displacements curves.

****
For guidelines on how to submit your revised manuscript please go the following address:
http://help.elsevier.com/app/answers/detail/p/7923/a_id/91

For further assistance, please visit our customer support site at http://help.elsevier.com/app/answers/list/p/7923 Here you can search for solutions on a range of topics, find answers to frequently asked questions and learn more about EES via interactive tutorials. You will also find our 24/7 support contact details should you need any further assistance from one of our customer support representatives.

Author's Response to Referee's Comments/Criticisms

General comments

The first paragraph under this heading is simply a copy of the Abstract of the Author's paper. Therefore, this is not a general comment.

The second paragraph is a general comment which is very favourable and publication is recommended with major revision. There is no explanation as to why the referee has chosen to use the adjective major. Moreover, the specific comments which are addressed below would seem to suggest that the adjective minor would be more appropriate!

Point 1)

The Author has cited Ascione et al's paper and added a few comments about it in the Introduction of the revised paper.

Point 2)

The Author has stated that the Wide Flange (WF) beam was pultruded by Strongwell. He has also added a few comments about the WF beam's fibreglass reinforcement (rovings and continuous filament mat) and the matrix (isophthalic polyester and filler). In addition, he has mentioned the approximate volume percentages of the constituents. He has pointed out that, as the paper is only concerned with the deflection serviceability limit response of continuous pultruded GFRP continuous beams, the important mechanical properties are the longitudinal elastic modulus and the shear modulus, which are given in Table 1 together with the beam's cross-section dimensions. He has also included a reference to Strongwell's EXTREN® design manual where strength values are given. These would be required for an ultimate limit state analysis, but this does not form part of the present paper and, therefore, they are not included – reference to the design manual is deemed sufficient. The Author has also pointed out that all of the mechanical properties given in the design manual are minimum values, which may be significantly lower than the actual values.

Point 3)

The Author has included two multi-part figures (Figures 3 and 5) which comprise of several images of the loading and instrumentation.

As the loads are small at the deflection serviceability limit (3 kN and 1 kN for major- and minor-axis flexure, respectively), there were no visible cracks in the web-flange junction in either the loading or support zones which could have affected the beam's linear response. Indeed, Ascione's tests on I-section pultruded GFRP short span simply supported beams show that cracking in the web-flange junction zone does not arise until the mid-span deflection greatly exceeds 1/200th of the span (the deflection serviceability limit assumed in the paper).

Point 4)

The Author has clarified in the amended title (and elsewhere in the paper) that the paper deals with the deflection serviceability limit, not the ultimate limit state. Indeed, for the 3 m and 2 m spans of the present GFRP beam, the ultimate limit state is more likely to be failure by lateral buckling than either local buckling promoting rupture of the web-flange junction under the loading point. It is the Author's opinion that Ascione et al. were only able to witness ultimate failure in the latter mode because the span (1.18 m) of their simply supported beam was very short and its span to depth ratio (5.9) was very small.

Nowhere in the paper has the Author suggested that the beam's response would be linear up to failure. The two papers, one by Mosallam et al and the other by Feo et al., deal with the tensile strength of web-flange junctions of pultruded GFRP I-beams. The Author was not aware of the first paper, but was aware of Feo et al's paper, which cites several of the Author's papers on this topic . It is the Author's opinion that neither paper is relevant to the focus of the present paper. Consequently, progressive failure within the web-flange junction has not been considered.

Point 5)

The Author is at a loss to understand this comment! Figures 7 - 10 are load – displacement (deflections and rotations) graphs, showing the linear response at different locations along the pultruded GFRP continuous beam.

Note:-

The changes made to the paper to address the Referee's comments and criticisms are highlighted in red!

Cover Letter rev1.doc

Engineering Department,

Lancaster University,
Gillow Avenue,
Bailrigg,
Lancaster,
LA1 4YW.

9th January, 2016.

Professor Antonio Ferreira,
Editor,
Composite Structures.

Dear Antonio,

Exact Shear Deformation Analysis and Serviceability Testing of Pultruded GFRP Continuous Beams

Please would you kindly arrange for my revised paper, originally titled as above but now with a revised title, to be re-considered for publication in *Composite Structures*. It has not been submitted to any other journal for possible publication.

The revised title is:-

Testing and analysis of pultruded GFRP continuous beams for the deflection serviceability limit state

I look forward to receiving your decision on the revised paper's acceptability or otherwise for publication in due course.

Yours sincerely,

Geoff Turvey

Author's Response to Referee's Comments/Criticisms

General comments

The first paragraph under this heading is simply a copy of the Abstract of the Author's paper. Therefore, this is **not** a general comment.

The second paragraph is a general comment which is very favourable and publication is recommended with major revision. There is no explanation as to why the referee has chosen to use the adjective *major*. Moreover, the specific comments which are addressed below would seem to suggest that the adjective *minor* would be more appropriate!

Point 1)

The Author has cited Ascione et al's paper and added a few comments about it in the Introduction of the revised paper.

Point 2)

The Author has stated that the Wide Flange (WF) beam was pultruded by Strongwell. He has also added a few comments about the WF beam's fibreglass reinforcement (rovings and continuous filament mat) and the matrix (isophthalic polyester and filler). In addition, he has mentioned the approximate volume percentages of the constituents. He has pointed out that, as the paper is only concerned with the *deflection serviceability limit* response of pultruded GFRP continuous beams, the important mechanical properties are the longitudinal elastic modulus and the shear modulus, which are given in Table 1 together with the beam's cross-section dimensions. He has also included a reference to Strongwell's *EXTREN*® design manual where strength values are given. These would be required for an *ultimate limit state* analysis, but this does not form part of the present paper and, therefore, they are not included – reference to the design manual is deemed sufficient. The Author has also pointed out that all of the mechanical properties given in the design manual are *minimum* values, which may be significantly lower than the actual values.

Point 3)

The Author has included two multi-part figures (Figures 3 and 5) which comprise of several images of the loading and instrumentation.

As the loads are small at the deflection serviceability limit (3 kN and 1 kN for major- and minor-axis flexure, respectively), there were no visible cracks in the web-flange junction in either the loading or support zones which could have affected the beam's linear response. Indeed, Ascione's tests on I-section pultruded GFRP short span simply supported beams show that cracking in the web-flange junction zone does not arise until the mid-span deflection greatly exceeds 1/200th of the span (the deflection serviceability limit assumed in the paper).

Point 4)

The Author has clarified in the amended title (and elsewhere in the paper) that the paper deals with the *deflection* serviceability limit, **not** the *ultimate limit state*. Indeed, for the 3 m and 2 m spans of the present GFRP beam, the ultimate limit state is more likely to be failure by lateral buckling than either local buckling promoting rupture of the web-flange junction under the loading point. It is the Author's opinion that Ascione et al. were only able to witness ultimate failure in the latter mode because the span (1.18 m) of their simply supported beam was very short and its span to depth ratio (5.9) was very small.

Nowhere in the paper has the Author suggested that the beam's response would be linear up to failure. The two papers, one by Mosallam et al and the other by Feo et al., deal with the tensile strength of web-flange junctions of pultruded GFRP I-beams. The Author was not aware of the first paper, but was aware of Feo et al's paper, which cites several of the Author's papers on this topic . It is the Author's opinion that neither paper is relevant to the focus of the present paper. Consequently, progressive failure within the web-flange junction has not been considered.

Point 5)

The Author is at a loss to understand this comment! Figures 7 - 10 are load – displacement (deflections and rotations) graphs, showing the linear response at different locations along the pultruded GFRP continuous beam.

<u>Note</u>:-

The changes made to the paper to address the Referee’s comments and criticisms are highlighted in red!

Testing and analysis of pultruded GFRP continuous beams for the deflection serviceability limit state

by

G.J. Turvey

Engineering Department, Lancaster University, Gillow Avenue, Lancaster, LA1 4YN

Abstract

An investigation of the deformation response of an unequal two-span pultruded glass fibre reinforced polymer (GFRP) wide flange (WF) beam up to the deflection serviceability limit is described. The beam was subjected to vertical point loading at the centre of the longer span. Mid-span deflections, support rotations and outer surface flange strains recorded during major- and minor-axis flexure tests on the beam are presented and shown to be both repeatable and linear. New closed-form shear deformation equations are presented for the forces and displacements of two-span continuous beams of arbitrary span ratio with the longer span subjected to a vertical mid-span point load. The equations have been used to predict the mid-span deflections, support rotations and surface strains recorded during the flexure tests. It is shown that the equations are able to predict the experimental deflections accurately. Depending on the particular support, the rotations (particularly the minor-axis rotations) are slightly under/over-estimated and, in general, the surface strains are over-estimated. It is concluded that this investigation provides further confirmation of the utility of shear deformation continuous beam equations for predicting the deformations of pultruded GFRP beams up to the deflection serviceability limit.

Keywords: GFRP; multi-span beams; pultrusions; serviceability deformations; shear-deformation analysis; testing

1. Introduction

Published research on the flexural analysis and testing of pultruded glass fibre reinforced polymer (GFRP) beams dates from the late 1980s. A particular focus of some of this early research was on symmetric three/four-point flexure tests of single-span simply supported beams in order to characterise the longitudinal elastic flexural and shear moduli of their cross-sections (see, for example, [1] and [2]). Indeed, this type of investigation has been continuing almost up to the present day with minor changes to the loading configurations being proposed (see, for example, [3] and [4]). Perhaps the most effective new load test for the determination of the longitudinal elastic flexural and shear moduli of pultruded GFRP beams is that given in [5].

Other early research on the static flexural analysis and testing of pultruded GFRP single-span beams has been reported in [6] – [9]. Subsequently, analyses of symmetrically loaded single-span pultruded GFRP beams with semi-rigid end connections (see, for example, [10] and [11]) have been reported, followed by analytical and experimental studies of the flexural stiffening effects of carbon fibre reinforced polymer (CFRP) strips bonded to the flanges of pultruded GFRP beams with semi-rigid end connections [12]. Hai et al [13] also carried out four-point symmetric loading tests on simply supported single-span glass-carbon, i.e. hybrid fibre reinforced polymer (HFRP), beams and used FE analysis to simulate their load – deflection responses and to identify the near optimal carbon to glass ratios in the beams' flanges. Most recently, Ascione et al. [14] reported failure (*ultimate* limit state) tests on four very short (1.18 m) span simply supported pultruded GFRP I-beams as part of an investigation to assess the benefits of fabricating such beams from an assembly of bonded pultruded GFRP plates.

The studies cited above relate to flexural tests on single-span beams subjected to symmetric concentrated loading with both ends, simply, semi-rigidly or rigidly supported. That said, analyses and tests have also been reported on tip-loaded cantilevered pultruded GFRP beams with and without CFRP flange stiffening [15].

By contrast to the growing number of analytical and experimental investigations reported on single-span pultruded GFRP and CFRP-stiffened/HFRP beams, the number of investigations reported on the flexural response of pultruded GFRP continuous beams is scant. It appears that Keller and de Castro [16] were probably the first to carry out such analysis and testing of pultruded GFRP beams. They tested equal two-span pultruded

GFRP box-section beams to failure under patch loading applied symmetrically about the central support. More recently, Turvey [17] reported deflection serviceability limit tests on equal two-span pultruded GFRP wide-flange (WF) beams subjected to symmetric mid-span point loading and demonstrated that deflections, support rotations and surface strains could be predicted reasonably accurately using exact shear-deformable beam theory.

The present paper seeks to extend the analytical work in [17] by presenting exact shear deformation equations for unequal two-span continuous beams subjected to vertical point loading applied at the centre of the longer span and to demonstrate their accuracy by comparison with tests on pultruded GFRP WF beams with respect to both their major- and minor-axes of flexure.

By way of achieving the foregoing objectives, the Method of Influence Coefficients [18] - used to derive the closed-form equations - is outlined briefly. Thereafter, the equations for the forces and displacements are presented for the case of the longer span supporting a vertical mid-span point load.

The experimental part of the investigation begins with details of the pultruded GFRP WF beam's cross-section geometry and its longitudinal elastic and shear moduli. An explanation of the unequal two-span beam test setup then follows and the instrumentation for recording deformations and forces is described. The loading procedure for both major- and minor-axis tests is explained, followed by demonstrations of the repeatability of the beam's load – deformation responses. Comparisons are then presented of the predicted and observed responses of the continuous beam and conclusions are drawn as to the accuracy and validity of the closed-form equations for predicting the deflection serviceability limit response.

2. Outline derivation of the exact shear-deformable continuous beam equations

Figure 1 shows the geometry of a two-span continuous beam supporting a vertical point load at the centre of the longer span L. The shorter, unloaded span is of length $\mu L\left(\mu \le 1\right)$. The longitudinal elastic modulus and shear modulus of the beam's doubly symmetric cross-section are denoted by E and G, respectively. Likewise, the area and second moment of area of the beam's cross-section are denoted by A and I, respectively. The beam supports a vertical point load W at D, the centre of the longer span. Accordingly, the reactions R_A, R_B and R_C at the each of the simple supports, A, B and C, respectively act in the directions shown in Figure 1.

Clearly, the beam in Figure 1 is statically indeterminate to the first degree. The choice of redundant action, which must be determined before the analysis can progress, is arbitrary. There is, however, benefit to be gained, through analysis simplification, by selecting this action as the internal moment at the support C. Thus, the procedure followed is to introduce a release (a pin joint) at support C. Two bending moment and shear force sub-systems are then set up – one for the load W acting on the released structure and the other for equal and opposite unit couples, acting at C, on the released structure. The bending moment (m) and shear force (s) distributions corresponding to the first and second sub-systems are distinguished by the subscripts 0 and 1, respectively. It may be shown (see [18] for further details), that the equation for the two sub-systems, which restores the displacement continuity (compatibility) at C in the original system can be expressed as:-

$$X\mu_{10} + f_{11} = 0 \qquad (1)$$

In Eq.(1) μ_{10} is the load coefficient, f_{11} is the influence coefficient and X is the internal moment at the support C. The load and influence coefficients are determined by integrating the bending moment and shear force distributions (divided by EI and GA, respectively) over the entire span of the beam for each of the two sub-systems. Thus, μ_{10} and f_{11} may be expressed as:-

$$\mu_{10} = \int_0^{(1+\mu)L} m_0 \frac{m_1}{EI} dx + \int_0^{(1+\mu)L} s_0 \frac{s_1}{GA} dx \qquad (2)$$

and

$$f_{11} = \int_0^{(1+\mu)L} m_1 \frac{m_1}{EI} dx + \int_0^{(1+\mu)L} s_1 \frac{s_1}{GA} dx \tag{3}$$

In Eqs.(2) and (3) x is the co-ordinate along the beam's centroidal axis and the integrals are evaluated stepwise graphically over the entire length of the continuous beam. μ_{10} and f_{11} are then substituted into Eq.(1) to determine the redundant action $X\left(=M_c\right)$.

Once the redundant action X has been determined, the displacements at A to E may be determined by applying Virtual Work (having set up bending moment and shear force diagrams on the released structure corresponding to unit forces for each of the required displacements). Thus, for example, the equation for the deflection δ_D takes the following form:-

$$\delta_D = \int_0^{(1+\mu)L} m \frac{m_{\delta_D}}{EI} dx + \int_0^{(1+\mu)L} s \frac{s_{\delta_D}}{GA} dx \tag{4}$$

where

$$m = m_0 + X m_{\delta_D} \; ; \; s = s_0 + X s_{\delta_D} \tag{5a - b}$$

and m_{δ_D} and s_{δ_D} are the bending moment and shear force distributions (of the second sub-system) for the unit vertical force applied at D.

Having, set up in turn the bending moment and shear force diagrams for unit values of the forces corresponding to each of the displacements, δ_D, δ_E, θ_A, θ_B and θ_C and evaluating integrals similar to those in Eq.(4) using expressions similar to those in Eqs.(5a - b), the required closed-form formulae for the two deflections and three support rotations may be established.

The force and displacement equations accounting for shear deformation for the continuous beam shown in Figure 1 are:-

$$R_A = \frac{W}{16}\left[\frac{\left\{\mu(5+8\mu)+24(1+\mu)\alpha\right\}}{(1+\mu)(\mu+3\alpha)}\right] ; \; R_C = \frac{W}{16}\frac{\left[(3+8\mu)+24\alpha\right]}{(\mu+3\alpha)} ;$$

$$R_B = \frac{3W}{16}\left[\frac{1}{(1+\mu)(\mu+3\alpha)}\right] = \frac{M_C}{\mu L} \tag{6a - d}$$

$$\delta_D = \frac{WL^3}{768EI}\left[\frac{\mu(7+16\mu)+48\alpha(1+\mu)(1+4\mu+12\alpha)}{(1+\mu)(\mu+3\alpha)}\right]; \; \delta_E = \frac{-3WL^3}{256EI}\left[\frac{\mu^3}{(1+\mu)(\mu+3\alpha)}\right] \tag{7a - b}$$

$$\theta_A = \frac{WL^2}{32EI}\frac{(1+2\mu)(\mu+6\alpha)}{(1+\mu)(\mu+3\alpha)} ; \; \theta_C = \frac{WL^2}{16EI}\frac{\left(\mu^2+3\alpha\right)}{(1+\mu)(\mu+3\alpha)} ; \; \theta_B = -\frac{WL^2}{32EI}\frac{\left(\mu^2-6\alpha\right)}{(1+\mu)(\mu+3\alpha)} \tag{8a - c}$$

In Eqs. (6 - 8) the parameter $\alpha\left(=\frac{EI}{GAL^2}\right)$ is the dimensionless shear-flexibility of the pultruded GFRP beam.

A shear correction factor k can readily be included in the denominator of the expression for α, if required.

3. Major- and minor-axis flexure tests on an unequal two-span continuous pultruded GFRP WF beam

In order to check the validity/utility of the closed-form equations presented in Section 2, load - deformation tests should be carried out on beams loaded in accordance with Figure 1. An *EXTREN® 500 Series* pultruded GFRP WF beam manufactured by Strongwell [19] was selected for these tests. The beam incorporates E-glass reinforcement in two forms: (1) rovings (bundles of parallel fibres) form the longitudinal reinforcement and (2) continuous filament mat (CFM) forms the transverse reinforcement. The roving and CFM layers alternate through the thickness of the flanges and the web with the CFM forming the outer layers. The outer surfaces of the flanges and web are formed by surface veils (lightweight CFM layers) which promote resin rich surfaces and facilitate safe manual handling of the profiles. The resinous matrix which encapsulates and, when cured, rigidizes the glass fibres is a mixture of isophthalic polyester resin and inert filler (kaolin or calcium carbonate). The volume percentages of glass fibre, resin and filler in the EXTREN® 500 series beams are typically of the order of 50, 40 and 10%, respectively Details of the beam's cross-section geometry, together with its longitudinal elastic and shear moduli, which are required for the present one-dimensional deflection serviceability limit state analysis are given in Table 1. Additional material properties, e.g. the longitudinal tensile and flexural strengths etc., which would be needed for an ultimate limit state analysis, may be found in [19]. However, it should be appreciated that the material property values given in the latter document are *minimum* values and that the actual values measured in tests may be considerably higher.

The experimental setup for the serviceability load – deflection tests was selected such that the lengths of the longer and shorter spans were 3m and 2 m, respectively, as shown in Figure 2.

The beam was instrumented with a vertical dial gauge in contact with its soffit at each of the mid-span positions, D and E. Each dial gauge had a 50 mm travel and a displacement resolution of 0.01 mm. An image of a dial gauge in contact with the beam's soffit at a mid-span position is shown in Figure 3(a). In addition, a clinometer was fastened to one face of the beam's web at the mid-depth position above each of the roller supports at A, B and C. Likewise, an image of a clinometer attached to the beam's web at one of the simply supported ends is shown in Figure 3(b). The clinometers had a rotation resolution of 0.001^{o} over the first few degrees of their rotation range. Furthermore, three sets of strain gauges were bonded to the outer surfaces of the beam's flanges. An image of a pair of strain gauges bonded near to the outer edges of the top flange of the beam is shown in Figure 3(c). Because the continuous beam had been tested previously with equal 2.5 m spans under symmetric mid-span point loading, the strain gauge layouts did not coincide with the cross-sections at D, C and E for the load - deformation tests. The locations and distributions of the gauges are shown in Figure 4 for the major-axis flexure tests. All of the strain gauges were uniaxial with 10 mm gauge lengths and 120 Ω internal resistances. The sensitive axes of the gauges were parallel to beam's longitudinal axis and were inset 10 mm from the free edges of the flanges to minimise the effects of any internal wrinkling of the fibre architecture close to the edges.

The beam was loaded by means of a manually operated 50 kN capacity hydraulic jack bolted to a steel reaction frame. The load was monitored via the readout from a 10 kN capacity load cell located between the end of the jack's ram and a steel ball joint bonded to the middle of the beam's top flange at the centre of the longer span (location D in Figure 2). Images of the point load arrangement on the top flange and the jack with the load cell attached to the end of its ram are shown in Figures 5(a) and 5(b), respectively.

The beam was tested first in major-axis flexure under load control. The load was applied in 0.2 kN increments and after each increment the deflections at D and E and the rotations at A, C and B were recorded. When the load reached 3 kN, the deflection at D was approximately 15 mm (corresponding to a serviceability deflection limit of $1/200^{th}$ of the longer span). The beam was then unloaded in 0.2 kN decrements. This load – unload test sequence was repeated three times. During the first, second and third load – unload tests only the strains of gauges G1 – G4, G7 – G10 and G5 – G6, respectively were recorded. Consequently, only the repeatability of deflections and rotations could be established during these tests.

After the major-axis tests had been completed, the beam was rotated through 90^{o} about its longitudinal axis, so that it could be prepared for testing with respect to its minor-axis. Several minor modifications had to be made so that the beam could be loaded through the top edges of its flanges and the clinometers and dial gauges had to be re-positioned. Figure 6 shows the locations and orientations of the strain gauges for the minor-axis flexural tests. Again, the beam was subjected to three load – unload tests. The load increments/decrements and the maximum load were reduced to 0.1 kN and 1 kN, respectively. During each test deflections and rotations were again recorded after each load increment/decrement up to a maximum deflection at D of approximately 15 mm. The strain gauge readings were recorded following the same sequence as in the major-axis tests.

4. Repeatability of major- and minor-axis load - deformation responses

The load versus deflection responses for the mid-spans of the longer and shorter spans of the beam tested in major- and minor-axis flexure are shown in Figures 7(a) and 7(b) respectively. It is evident that the repeatability of the mid-span deflections is excellent for the major-axis tests. For the minor-axis tests the repeatability of the deflection at the mid-span of the longer span is not quite as good for the lower loads, but is excellent for the mid-span of the shorter span.

The repeatability of the support rotations for major- and minor-axis flexure are shown in Figures 8(a) and 8(b) respectively. Again, it is evident that the rotations for both major- and minor-axis flexure are consistent and repeatable. It should be appreciated that the magnitudes of the rotations shown in Figures 8(a) and 8(b) for the corresponding supports are very similar. This is not altogether surprising because the beam was loaded up to the same maximum deflection (approximately 15 mm) at the centre of the longer span for both the major- and minor-axis flexure tests. However, to achieve this, the maximum load applied in the major-axis tests was three times that in the minor-axis tests.

5. Comparison of the experimental and theoretical deformations and strains

The theoretical deformations have been determined from Eqs. 7(a-b) and 8(a-c) using the following values from Table 1:-

$E = 21.4 GPa$, $G = 3 GPa$, $A_g = 1.845x10^3\ mm^2$, $I_{maj} = 3.30x10^6\ mm^4$, $I_{\min} = 1.10x10^6\ mm^4$, $L = 3m$ and $\mu = 0.667$.

In addition, the values of the dimensionless shear flexibility parameter α for the major- and minor-axis bending calculations were determined as $1.40x10^{-3}$ and $6.71x10^{-4}$, respectively. Since the theoretical deformations are linear functions of the applied load, it was only necessary to use the maximum loads applied in the major- and minor-axis flexure tests, namely 3 kN and 1 kN respectively, in order to define the dashed straight lines in Figures 9 and 10.

The results for the mid-span deflections obtained from Test 3 of the major- and minor-axis beam tests are compared in Figures 9(a) and 9(b) respectively with the theoretical deflections obtained from Eqs. 7(a) and 7(b) using the data given above. It is evident, as shown in Figure 9(a), that the theoretical mid-span deflections slightly over-predict the deflections obtained from the third major-axis flexure test at the highest loads. On the other hand, for the minor-axis flexure tests shown in Figure 9(b), the agreement between the Test 3 mid-span deflections and the theoretical deflections is excellent.

Comparisons of the experimental and predicted rotations at the supports A, B and C are shown in Figure 10(a) and 10(b) for major- and minor-axis flexure, respectively. It is evident that the support rotations predicted using Eqs. 8(a –c) agree more closely with the rotations measured in the third major-axis beam test than those measured in the minor-axis beam test. More specifically, it appears that the experimental rotations are: (1) under-estimated at support A for both major- and minor-axis flexure, (2) over- and under-estimated for major- and minor-axis flexure, respectively, at support B and (3) in very good agreement for major-axis flexure and under-estimated for minor-axis flexure at support C.

The theoretical flexural strains ε on the surfaces of the beam's flanges at the locations in the longer and shorter spans (see Figures 4 and 6) were calculated using simple bending theory,

$$\varepsilon = \pm \frac{My}{IE} \tag{9}$$

In Eq. (9) the bending moment M at each location was evaluated according to the following:-

$$M = 1.25 R_A \left[Nm \right] \text{ (strain gauges G1 - G4)}$$

$$M = \frac{1}{2}\left(5R_A - 2W\right)\left[Nm\right] \text{ (strain gauges G5 and G6)}$$

$$M = 1.25R_B\,[Nm] \text{ (strain gauges G7 – G10)}$$

In addition, the second moments of area I and distances y from the neutral axis to the centre lines of the strain gauges were evaluated as:-

$$I = I_{maj}\left[m^4\right] \text{ and } y = \frac{d}{2}\left[m\right] \text{ (major-axis flexure)}$$

$$I = I_{\min}\left[m^4\right] \text{ and } y = \frac{1}{2}\left(d - 0.02\right)\left[m\right] \text{ (minor-axis flexure)}$$

The experimental and theoretical strains recorded by gauges G1 – G4 are shown in Figures 11(a) and 11(b) for major- and minor-axis flexure, respectively. It is evident that the agreement between the compressive strains is not quite as good as that between the tensile strains for both major- and minor-axis flexure. Furthermore, the theoretical strains are greater than the experimental strains for major-axis flexure, but much less so for minor-axis flexure.

The comparison between experimental and theoretical strains for gauges G5 and G6 is shown in Figures 12(a) and 12(b) for major- and minor-axis flexure, respectively. During the major-axis test strain gauge G5 mal-functioned and, therefore, only the strains recorded by strain gauge G6 are compared with the theoretical strains in Figure 12(a). Given that the tensile strains are quite small, the theoretical strains agree well with the corresponding experimental values for major-axis flexure, though small under- and over-predictions of the experimental strains are evident at lower and higher loads respectively.

On the other hand, for minor-axis flexure, both gauges, G5 and G6, functioned satisfactorily and it is clear from Figure 12(b) that the theoretical strains slightly over-predict both the experimental compressive and tensile strains.

The theoretical – experimental strain correlations for strain gauges G7 – G10 (in the unloaded span) for major- and minor-axis flexure are shown in Figures 13(a) and 13(b), respectively. Again, it is evident for major-axis flexure that the tensile strains are in slightly better agreement than the compressive strains. Furthermore, the theoretical strains over-predict the experimental strains.

For minor-axis flexure, there is good agreement between the tensile strains, recorded by gauges G8 and G10, and the compressive strains, recorded by gauges G7 and G9. Furthermore, the theoretical tensile strains are in excellent agreement with the experimental tensile strains and the theoretical compressive strains only slightly over-predict the experimental compressive strains at the higher loads.

Concluding remarks

Major- and minor-axis flexure tests have been carried out on unequal two-span continuous pultruded GFRP beams with the longer span subjected to a vertical point load at its centre. The beams were loaded up to the serviceability deflection limit (approximately 15 mm for the longer 3 m span) and during the tests mid-span deflections and support rotations were recorded, together with longitudinal surface strains on the outer faces of the flanges. It has been shown that the deflections and rotations are repeatable and vary linearly with load.

The Influence Coefficient Method has been used to derive exact shear deformable equations for the forces $\left(R_A, R_B, R_C, M_C\right)$ and displacements $\left(\delta_D, \delta_E, \theta_A, \theta_B, \theta_C\right)$ for an unequal two-span beam of arbitrary span ratio $\left(\mu\right)$ when the longer span $\left(L\right)$ is subjected to a vertical point load $\left(W\right)$ at mid-span. The equations have been used to compute the mid-span deflections, support rotations and outer surface flange strains observed in the major- and minor-axis pultruded GFRP beam tests.

Comparisons of the experimental and theoretical deflections, support rotations and flange strains has shown reasonably good agreement for both major- and minor-axis flexure up to the serviceability deflection limit for the longer span.

The present investigation has, therefore, provided evidence, additional to that reported in [17], that elastic shear deformation beam theory is able to be used to predict the deformation response of pultruded GFRP beams with reasonable accuracy.

Acknowledgements

The author wishes to record his appreciation to Mr. J. Merlet, who undertook the beam tests under the author's direction during a Summer Internship in the Engineering Department. He also wishes to thank the staff of the Engineering Department, particularly Mr. M. Salisbury, for their support and assistance during the course of this investigation.

References

1. Sims GD, Johnson AF, Hill RD. Mechanical and structural properties of a GRP pultruded section. Composite Structures 1987; 8(3): 173-87.
2. Bank LC. Flexural and shear moduli of full-section fibre reinforced plastic (FRP) pultruded beams. Journal of Testing and Evaluation ASTM 1989; 17(1): 40-5.
3. Roberts TM and Al-Ubaidi H. Flexural and torsion properties of pultruded fiber reinforced plastic I-profiles. Journal of Composites for Construction 2002; 6(1): 28-34.
4. Barros da S, Santos Neto A, Lebre La Rovere H. Flexural stiffness characterisation of fiber-reinforced plastic (FRP) pultruded beams. Composite Structures 2007; 81(2): 274-82.
5. Minghini F, Tullini N and Laudiero F. Identification of the short-term full-section moduli of pultruded FRP profiles using bending tests. Journal of Composites for Construction 2014; 18(1): 04013030.
6. Barbero EJ. Pultruded structural shapes. SAMPE Journal 1991; 27(1): 25-30.
7. Davalos JF, Salim HA, Qiao P, Lopez-Anido R, Barbero EJ. Analysis and design of pultruded FRP shapes under bending. Composites Part B: Engineering 1996; 27(3-4): 295-305.
8. Nagaraj V, GangaRao HVS. Static behaviour of pultruded GFRP beams. Journal of Composites for Construction 1997; 1(3):120-9.
9. Kabir MZ, Sherburne AN. Shear strain effects on flexure and torsion of thin-walled pultruded composite beams. Canadian Journal of Civil Engineering 1999; 26(6): 852-68.
10. Turvey GJ. Analysis of pultruded GRP beams with semi-rigid end connections. Composite Structures 1997; 38(1-4): 3-16
11. Turvey GJ. Flexure of pultruded GRP beams with semi-rigid end connections. Composite Structures 2000; 47(1-4): 571-80.
12. Turvey GJ. Analysis of bending tests on CFRP-stiffened pultruded GRP beams. Proceedings of the Institution of Civil Engineers 2007; 160(SB1); 37-49.
13. Hai ND, Mutsuyoshi H, Asamoto S, Matsui T. Structural behaviour of hybrid FRP composite I-beams. Construction and Building Materials 2010; 24( ):956-69.
14. Ascione F, Mancusi G, Spadea S, Lamberti M, Lebon F, Maurel-Pantel A. On the flexural behaviour of GFRP beams obtained by bonding simple panels: an experimental investigation. Composite Structures 2015; 131:55-65.
15. Turvey GJ. Bending of tip-loaded CFRP stiffened pultruded GRP cantilevers: comparison between theory and experiment. Proceedings of the 13th European Conference on Composite Materials (ECCM 13), 2nd – 6th June 2008. Kungliga Tekniska Högskolan, Stockholm, Sweden [Session on Mechanical Properties. Paper 1202, pp.10 in CD-Rom Proceedings].
16. Keller T and de Castro J. System redundancy and ductility of FRP beam structures with ductile adhesive joints. Composites Part B: Engineering 2005; 36(8): 586-96.
17. Turvey GJ. Pultruded GFRP continuous beams – comparison of flexural test data with analysis predictions. Proceedings of the 5th International Conference on Advanced Composites in Construction. University of Warwick, 6th – 8th September 2011: 470-81.
18. Morice PB. Linear structural analysis: an introduction to the influence coefficient method applied to statically indeterminate structures. Thames and Hudson. London 1969.
19. Anon. Extren fiberglass structural shapes: design guide. Strongwell, Bristol, VA, 1989.

List of tables.doc

List of tables

Table 1: Geometry and elastic material properties of the pultruded GFRP WF beam used in the load – deformation tests

Table 1

Table 1 rev2.doc

Table 1

Geometry and elastic material properties of the pultruded GFRP WF beam used in the load – deformation tests

Cross-section Dimensions $\begin{Bmatrix} b \, x \, d \, x \\ t_f \left(= t_w\right) \end{Bmatrix}$# [mm]	Cross-sectional Area (A)		Second Moment of Area (I)		Average Elastic Longitudinal Modulus (E) [GPa]	Minimum Elastic Longitudinal Modulus (E) [GPa]	Elastic Shear Modulus (G) [GPa]
	Gross (A_g) [mm^2]	Web (A_w) [mm^2]	Major-axis (I_{maj}) [mm^4]	Minor-axis $(I_{\min})$ [mm^4]			
120 x120 x 6.4	1845	568	3.30 x 10^6	1.11 x 10^6	21.4*	17.2**	2.93**

*Average of four longitudinal coupon tests

** Manufacturer's minimum values

b, d, t_f and t_w are the breadth, depth, flange thickness and web thickness respectively

List of figures

Figure 1: An unequal two-span continuous beam loaded at the centre of the longer span.

Figure 2: Test setup for the serviceability load tests.

Figure 3(a): Dial gauge used to record the mid-span deflection of the beam's soffit.

Figure 3(b): Electronic clinometer attached to the beam's web to record the rotation at the simple support.

Figure 3(c): A pair of uniaxial strain gauges bonded to the beam's top flange to record its axial strain.

Figure 4: Positions of the uniaxial strain gauges along the beam loaded in major-axis flexure: (a) 1.25 m from A, (b) 2.5 m from A and (c) 1.25 m from B.

Figure 5(a): Steel ball joint bonded to the beam's upper flange at the mid-span loading point.

Figure 5(b): Load cell attached to the end of the jack's ram above the steel ball joint.

Figure 6: Positions of the uniaxial strain gauges along the beam loaded in minor-axis flexure: (a) 1.25 m from A, (b) 2.5m from A and (c) 1.25 m from B.

Figure 7: Repeatability of mid-span deflections: (a) major-axis tests and (b) minor-axis tests.

Figure 8: Repeatability of support rotations: (a) major-axis tests and (b) minor-axis tests.

Figure 9: Comparison of experimental and theoretical mid-span deflections: (a) major-axis flexure and (b) minor-axis flexure.

Figure 10: Comparison of experimental and theoretical support rotations: (a) major-axis flexure and (b) minor-axis flexure.

Figure 11: Comparison of experimental and theoretical surface strains for gauges 1 – 4: (a) major-axis flexure and (b) minor-axis flexure.

Figure 12: Comparison of experimental and theoretical surface strains for gauges 5 and 6: (a) major-axis flexure and (b) minor-axis flexure.

Figure 13: Comparison of experimental and theoretical surface strains for gauges 7 – 10: (a) major-axis flexure and (b) minor-axis flexure.

Figure 1

Figure 1.doc

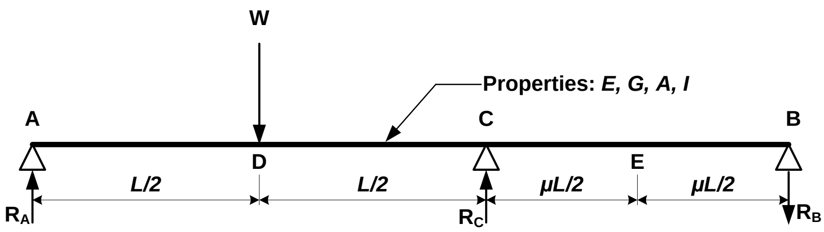

Figure 1

Figure 2

Figure 2.doc

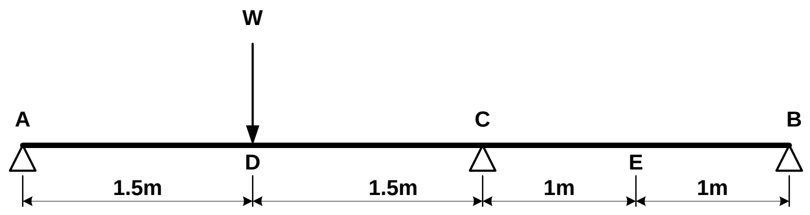

Figure 2

Figure 3(a)

Figure 3(a) rev2.doc

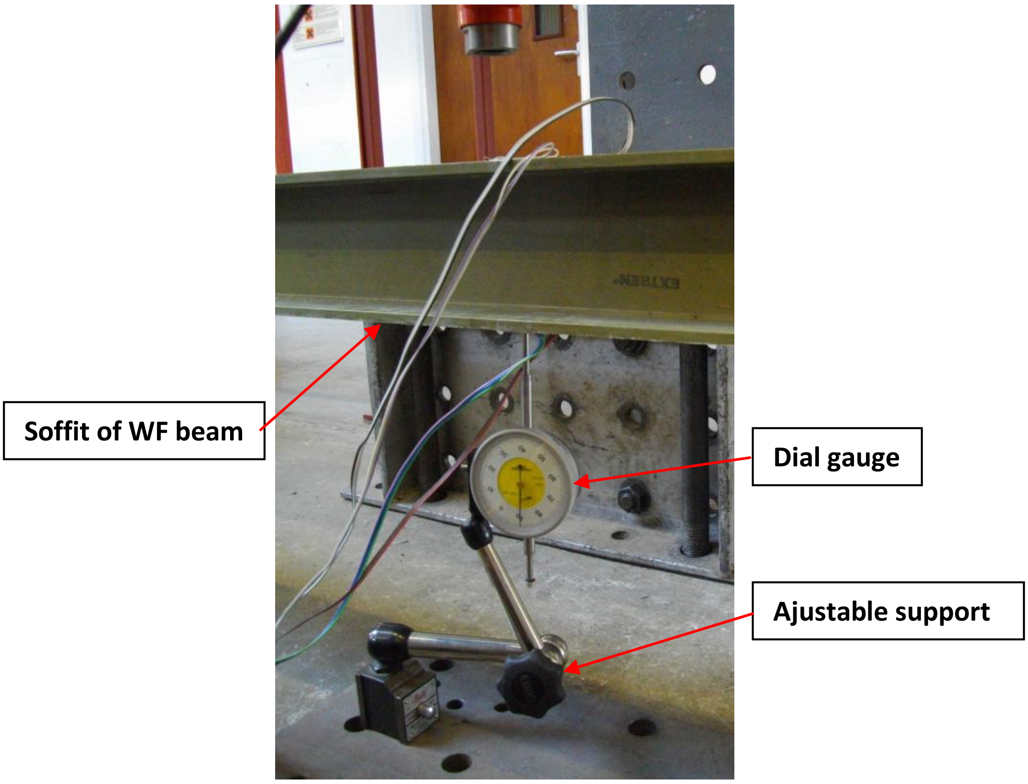

Figure 3(a)

Figure 3(a)

Figure 3(b) rev2.doc

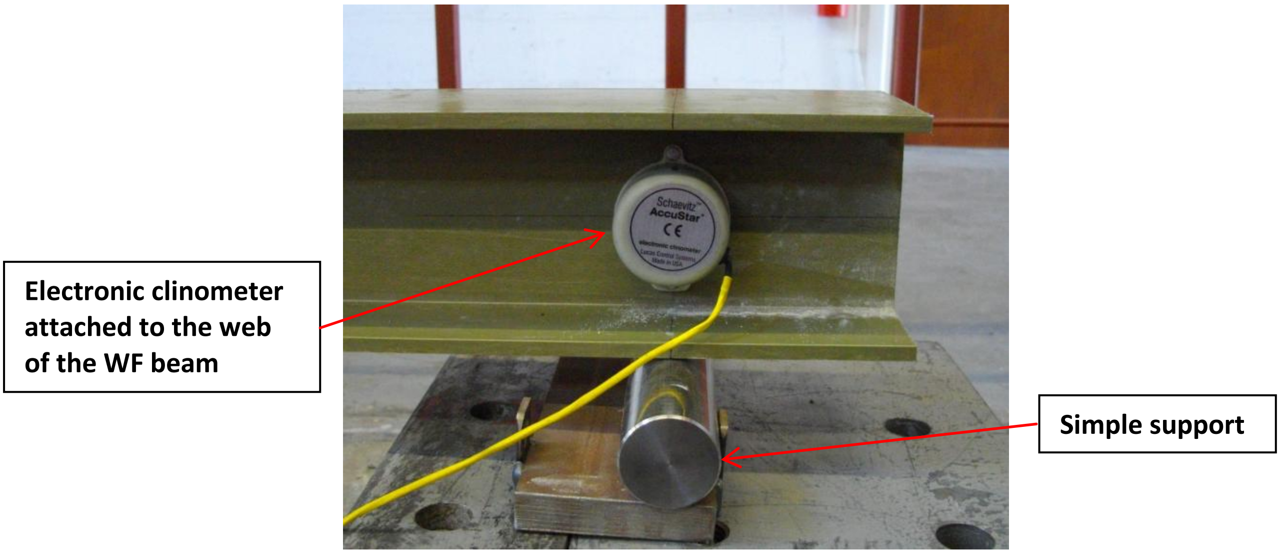

Figure 3(b)

Figure 3(c)

Figure 3(c) rev2.doc

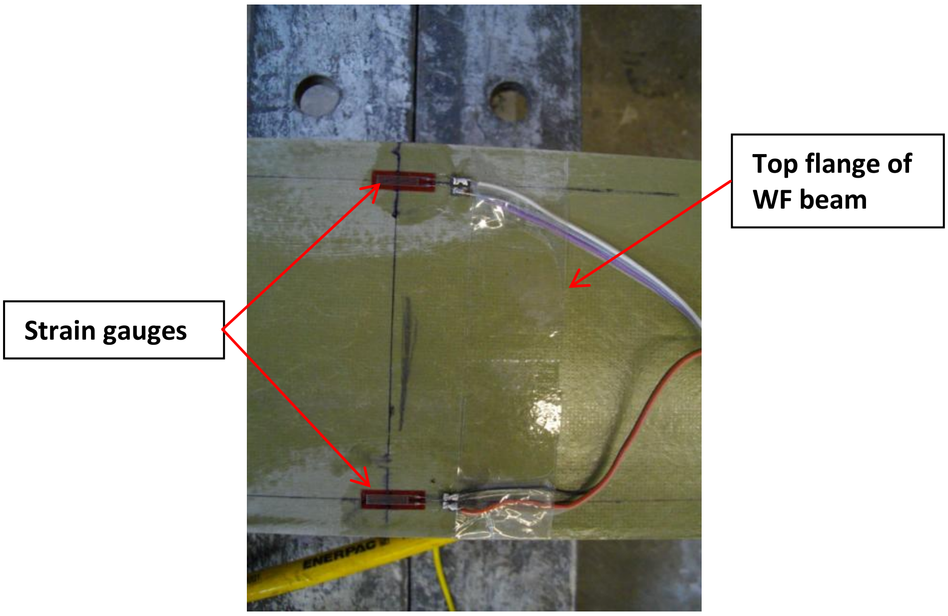

Figure 3(c)

Figure 4

Figure 4 rev1.doc

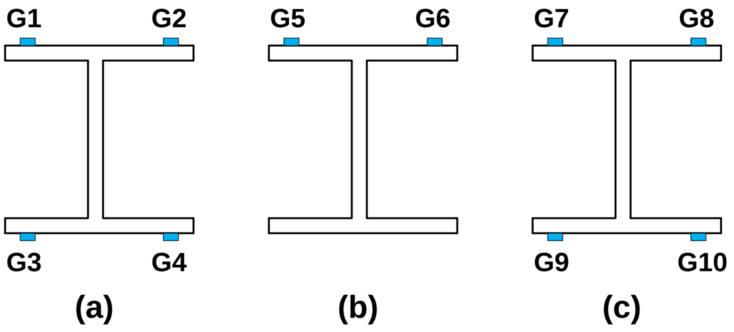

Figure 4

Figure 5(a)

Figure 5(a) rev4.doc

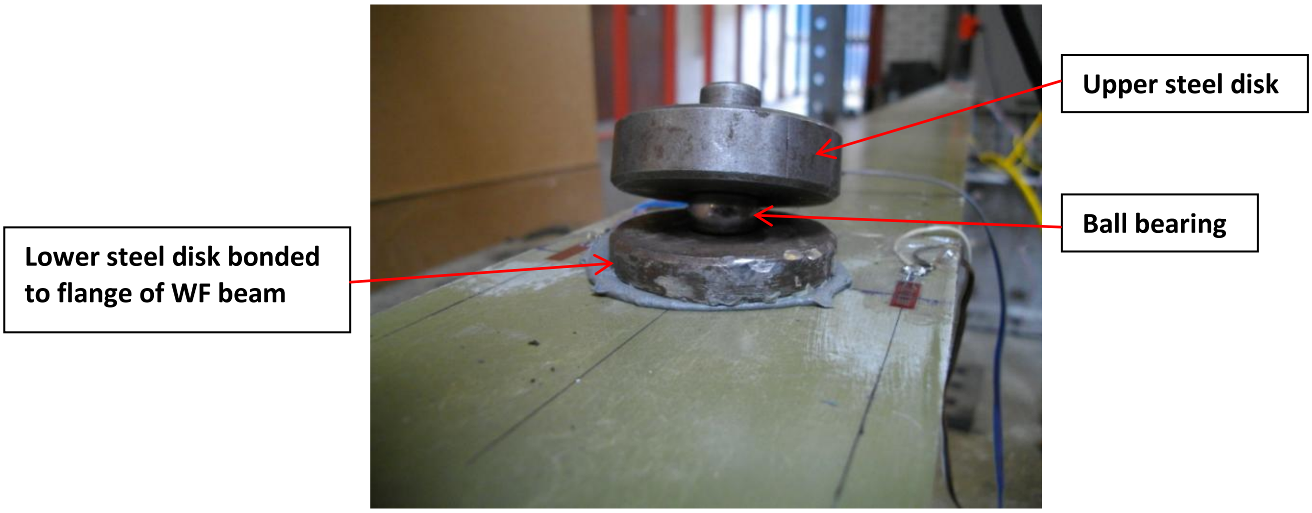

Figure 5(a)

Figure 5(b)

Figure 5(b) rev2.doc

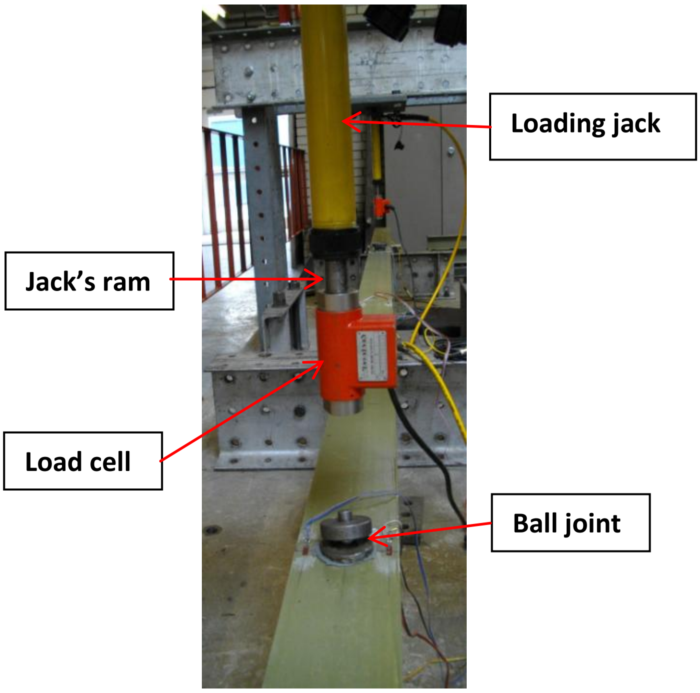

Figure 5(b)

Figure 6

Figure 6 rev1.doc

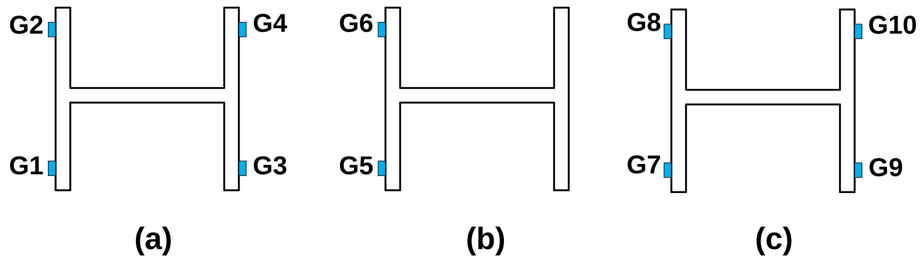

Figure 6

Figure 7(a)

Figure 7(a) rev1.doc

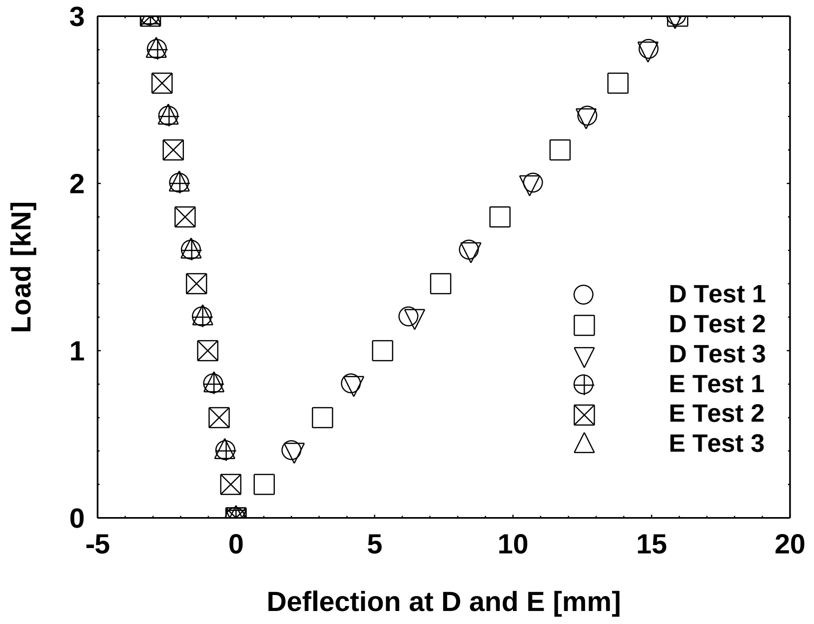

Figure 7(a)

Figure 7(b)

Figure 7(b) rev1.doc

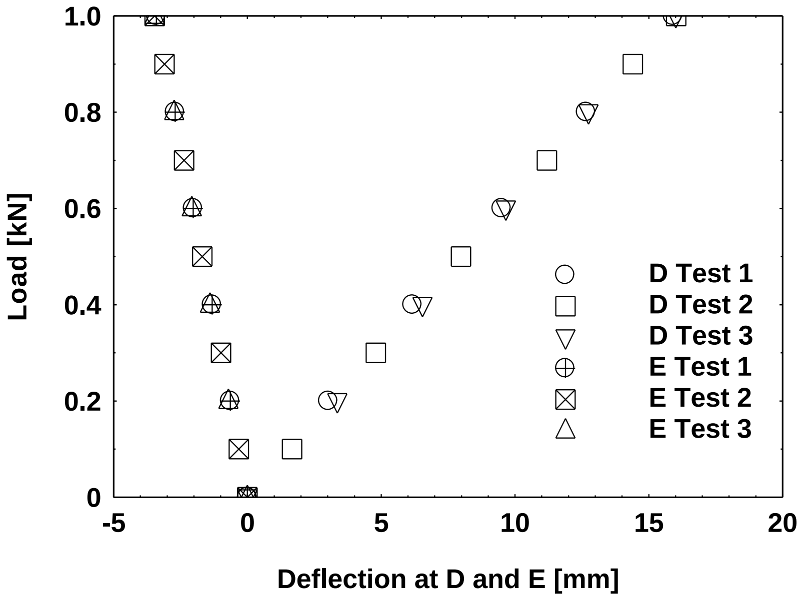

Figure 7(b)

Figure 8(a)

Figure 8(a) rev1.doc

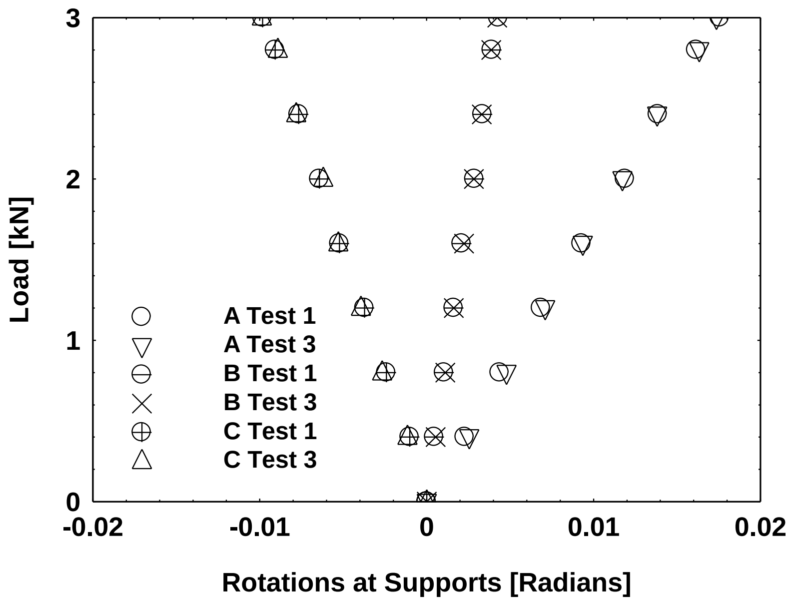

Figure 8(a)

Figure 8(b)

Figure 8(b) rev1.doc

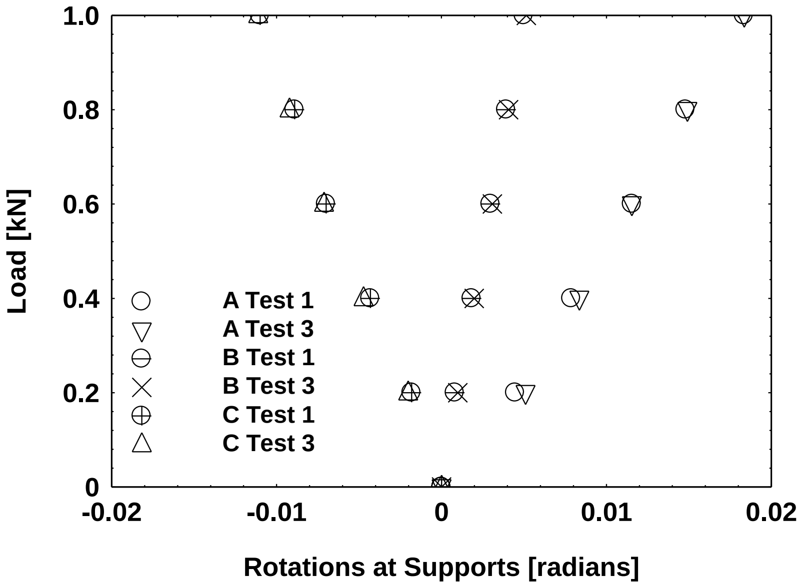

Figure 8(b)

Figure 9(a)

Figure 9(a) rev3.doc

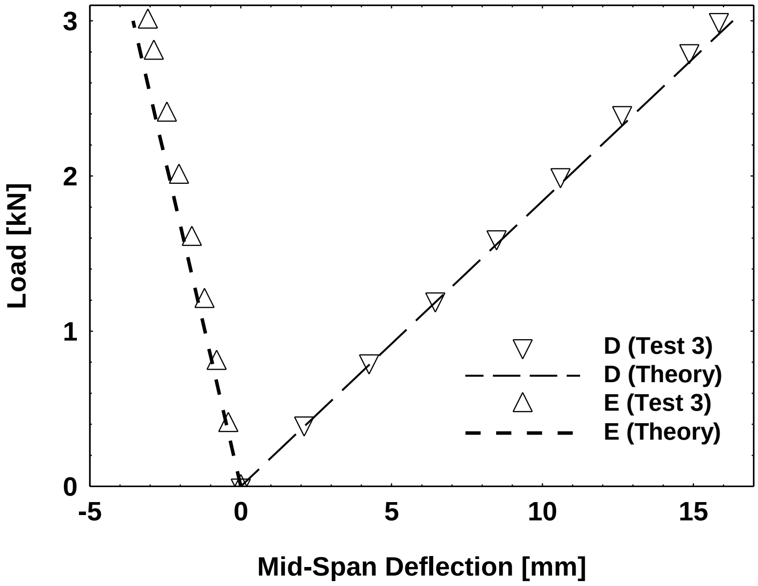

Figure 9(a)

Figure 9(b)

Figure 9(b) rev3.doc

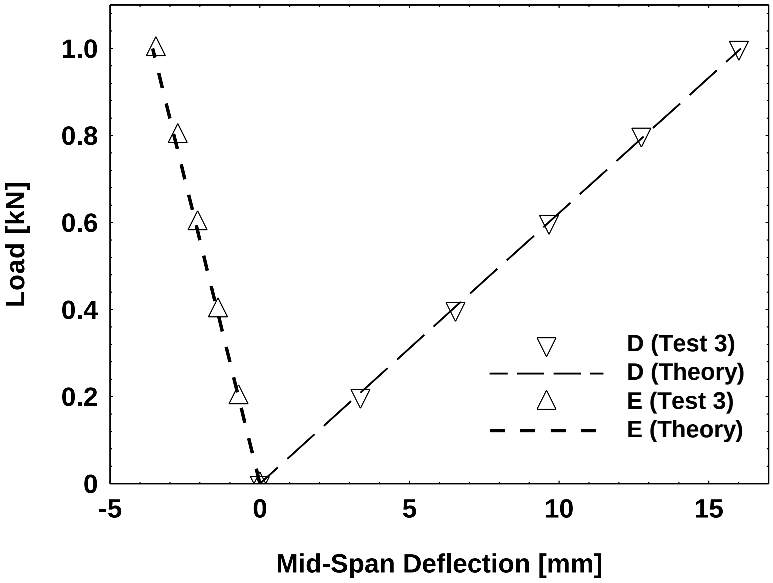

Figure 9(b)

Figure 10(a)

Figure 10(a) rev3.doc

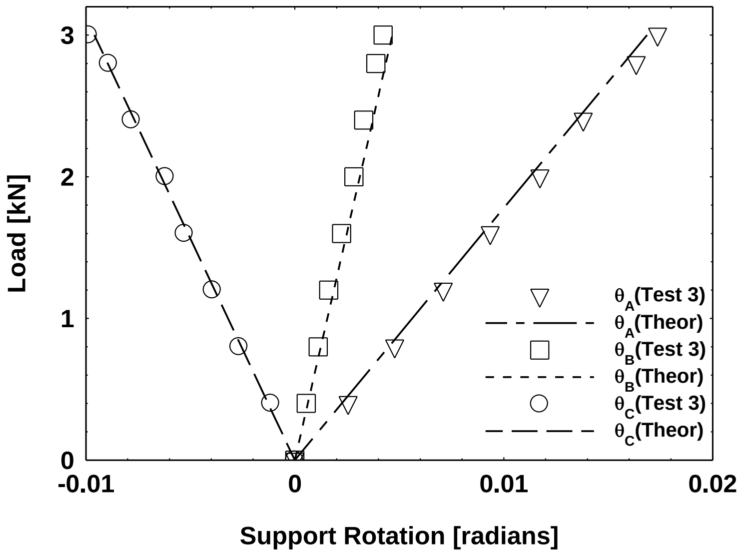

Figure 10(a)

Figure 10(b)

Figure 10(b) rev3.doc

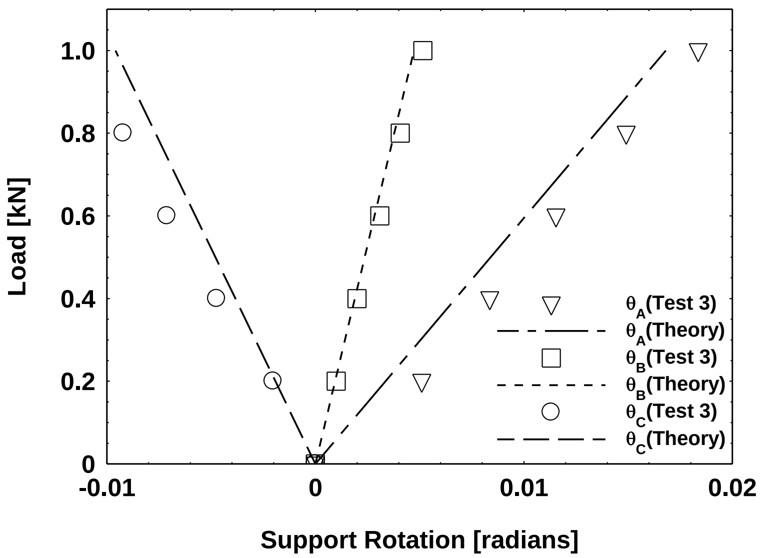

Figure 10(b)

Figure 11(a)

Figure 11(a) rev5.doc

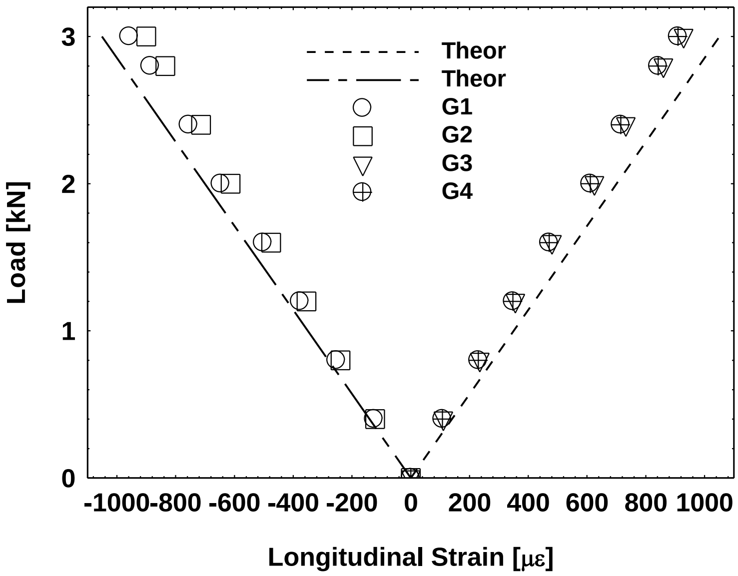

Figure 11(a)

Figure 11(b)

Figure 11(b) rev3.doc

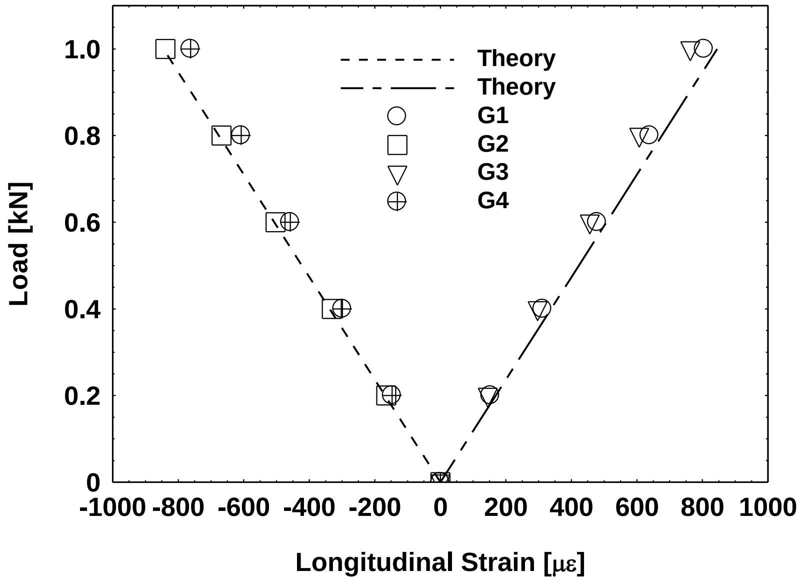

Figure 11(b)

Figure 12(a)

Figure 12(a) rev3.doc

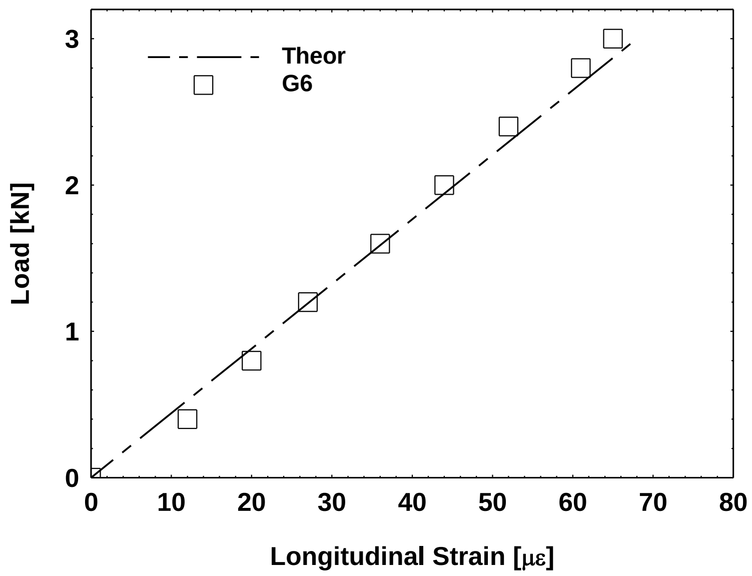

Figure 12(a)

Figure 12(b)

Figure 12(b) rev3.doc

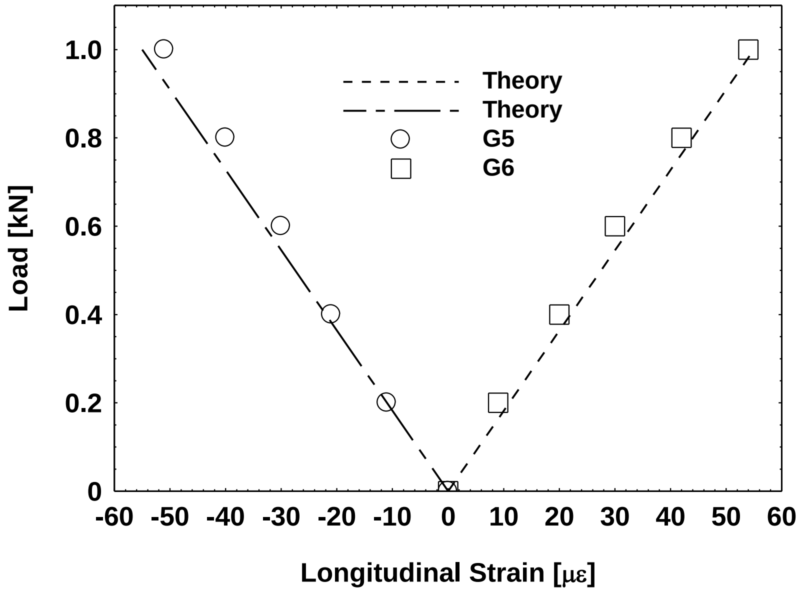

Figure 12(b)

Figure 13(a)

Figure 13(a) rev3.doc

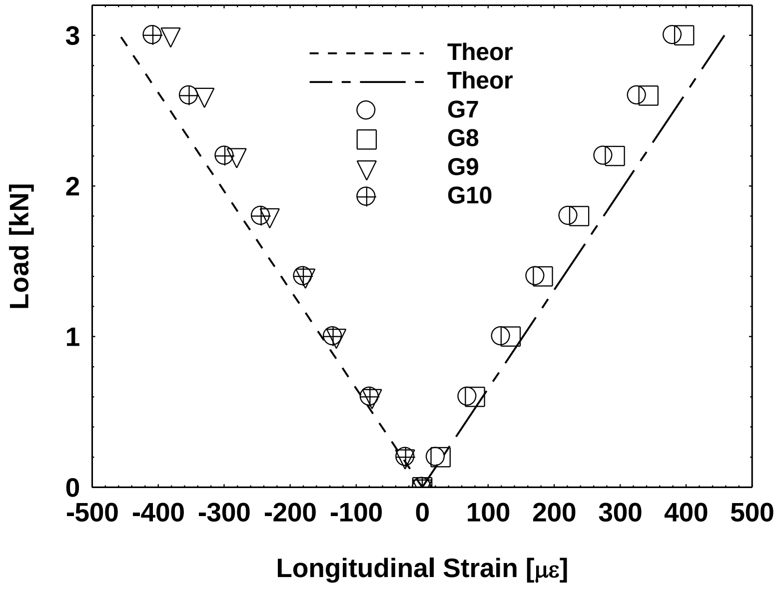

Figure 13(a)

Figure 13(b)

Figure 13(b) rev3.doc

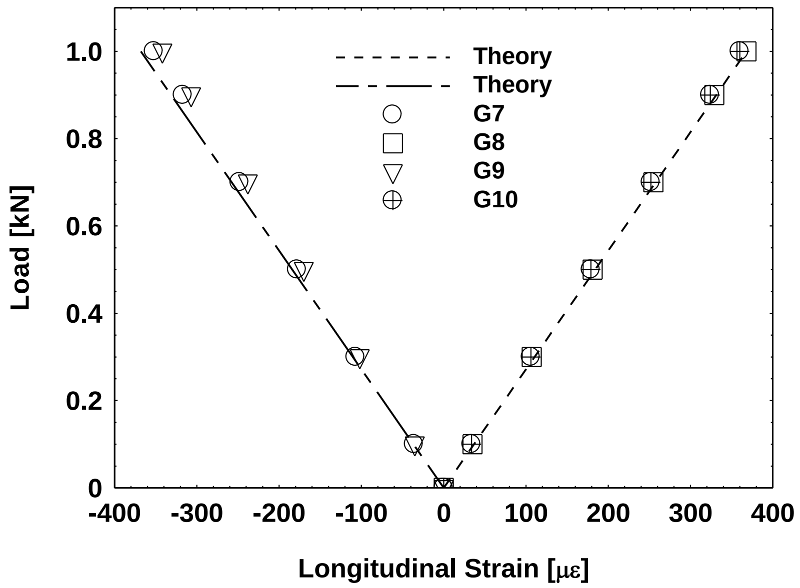

Figure 13(b)